Published in final edited form as:
Glia. 2008 March ; 56(4): 471–479. doi:10.1002/glia.20620.

Remodelling of motor nerve terminals in demyelinating axons of periaxin null mutant mice

Felipe A Court[1,2], **Peter J Brophy**[1], and **Richard R Ribchester**[1]

[1]Centre for Neuroscience Research, University of Edinburgh, Summerhall and George Square, Edinburgh EH8 9JZ, UK

Abstract

Myelin formation around axons increases nerve conduction velocity and regulates phenotypic characteristics of the myelinated axon. In the peripheral nervous system, demyelinating forms of hereditary Charcot-Marie-Tooth (CMT) diseases, due to Schwann-cell intrinsic molecular defects, leads to reduced nerve conduction velocity and changes in the axonal phenotype. Several mouse models of CMT diseases have been generated, allowing the study of consequences of demyelination in peripheral nerve fibres. Nevertheless, the effect of demyelination at the level of the neuromuscular synapse has been largely overlooked. Here we show that in the periaxin knock-out mice, a model of CMT condition, neuromuscular junctions develop profound morphological changes in pre-terminal region of motoraxons. These changes include extensive preterminal branches which originate in demyelinated regions of the nerve fibre and axonal swellings associated with residually-myelinated regions of the fibre. Using intracellular recording from muscle fibres we detected asynchronous failure of action potential transmission at high but not low stimulation frequencies, a phenomenon consistent with branch point failure. Taken together, our morphological and electrophysiological findings suggest that preterminal branching due to segmental demyelination near the neuromuscular synapse in periaxin KO mice may underlie phenotypic disabilities present in this mouse model of CMT disease. These results opens a new avenue of research in order to understand the cellular changes responsible for clinical disabilities in demyelinating conditions.

Introduction

Myelination of axons by Schwann cells and oligodendrocytes allows fast transmission of nerve impulses by insulating axonal segments, and restricting action potential regeneration to nodes of Ranvier, the non-myelinated axonal domains containing a high density of sodium ion channels. In addition to the role of the myelin sheath in the electrophysiological function of the nerve fibre, myelination regulates some structural and functional characteristics of the underlying axon, including its microtubule content, neurofilament phosphorylation, and axonal transport (de Waegh et al., 1992). The distribution of myelin further defines molecularly-distinct domains in the axolemma, including the localisation of

Address correspondence to: Dr. Felipe A. Court, Department of Physiological Sciences, Faculty of Biology, P. Universidad Católica de Chile, Av. B. O'Higgins 340, Santiago, Chile. Tel +56 2 686 ; fcourt@bio.puc.cl.
[2]Present address: Department of Physiological Sciences, Faculty of Biology, P. Universidad Católica de Chile, Av. B. O'Higgins 340 / Casilla 114-D, Santiago, Chile

Europe PMC Funders Author Manuscripts

K channels, caspr and neurofascin (Salzer, 2003). In addition, Schwann cells repress an intrinsic capacity of axons to sprout but the molecular mechanisms are unknown (Court and Alvarez, 2005). The regulatory properties of the myelin upon the axon are dramatically revealed in several clinical conditions in which phenotypic alterations of Schwann cells due to mutations in diverse Schwann cell-specific proteins leads, in addition to impairment in the electrophysiological capacity of nerve fibres, to a range of axonal pathologies including axonal swelling, defects in axonal transport and axonal degeneration (Bjartmar et al., 1999; Sancho et al., 1999; Krajewski et al., 2000; Martini, 2001).

One group of hereditary neuropathies produced by Schwann cell abnormalities that have been extensively studied due to their high incidence in the human population are Charcot-Marie-Thooth diseases (CMT). Several mouse models have been generated allowing a detailed study of the molecular mechanisms of CMT, their progression and phenotypic consequences (Martini, 1997; Zu Horste and Nave, 2006). Usual phenotypic characteristics of demyelinating forms of CMT (CMT1, 3 and 4) diseases are progressive reduction in nerve conduction velocity, muscle impairment and sensory dysfunction (Dyck and Thomas, 2005). In early stages of some human CMT conditions, reduction of nerve conduction velocity does not lead to overt clinical manifestation of the disease (Gutmann et al., 1983; Garcia et al., 1998), suggesting that other changes subsequently elicited by demyelination may produce the diagnostic clinical signs.

Until recently, one interesting and neglected possibility has been the effect demyelination may have at the level of the neuromuscular junction (NMJ). In intramuscular nerve fibres, myelination extends proximal to the last pre-terminal branch point of an axon innervating the muscle fibre. Thus, demyelination in this region could lead to structural changes at the neuromuscular junction with important electrophysiological consequences. Evidence of secondary neuromuscular defects has been obtained in studies of mice overexpressing the myelin protein zero (P0), in which myelin sheath formation is significantly impaired (Yin et al., 2004). Neuromuscular junctions also show abnormalities even though P0 is not expressed in motor neurones either normally or in the overexpressing transgenics (Wrabetz et al., 2000). However, similar studies in progressive demyelinating conditions have not been reported so far.

In order to understand the possible contribution of morphological and electrophysiological changes at the NMJ to the phenotype of demyelinating conditions we examined muscles in periaxin null mutant mice.

Periaxin is expressed by myelinating Schwann cells and associates with the dystroglycan complex through Drp2 (Sherman et al., 2001) at the abaxonal region of the cell. Periaxin null mutant mice develop a late-onset peripheral nerve demyelinating condition (Gillespie et al., 2000). These mice represent an accessible model of the human CMT4A condition, in which mutations in the molecular homologue of periaxin has been identified (Guilbot et al., 2001; Takashima et al., 2002; Kabzinska et al., 2006). Here we show that pre-terminal demyelination leads to morphological changes in the arborisation pattern of motoraxons approaching the NMJ, with consequential defects in neuromuscular transmission during repetitive nerve stimulation.

Results

Periaxin is expressed in myelinating Schwann cells but not in terminal ones

In peripheral nerve, periaxin is exclusively expressed by myelin-forming Schwann cells (Gillespie et al., 2000). In order to asses periaxin expression at the neuromuscular junction, triangularis sterni (TS) muscles from wild-type (WT) mice were immunostained using an antibody against periaxin together with fluorescent conjugates of α–bungarotoxin (α–BTX) to stain postsynaptic acetylcholine receptors (AchR) at motor endplates. As shown in Figure 1A, periaxin is expressed by myelin-forming Schwann cells located in pre-terminal regions and intramuscular nerve fibres but not in terminal Schwann cells capping the neuromuscular synapse. As expected, periaxin null mice (prx−/−) TS muscles shown complete absence of periaxin immunoreactivity (Figure 1B).

Demyelination of nerve fibres produces morphological abnormalities at NMJ

Peripheral demyelination in prx−/− is first detected at around 2 months of age and progresses to a severe condition during the following months, phenotypically characterised by muscle weakness, tremor and sensory abnormalities (Gillespie et al., 2000). Peripheral nerve fibres from 8-month old periaxin null mice present extensive demyelinated axonal segments that contrast with the regular myelination in WT fibres interrupted only at the nodal gap (Fig. 2A and B and (Gillespie et al., 2000)). In addition, prx−/− nerve fibres exhibit supernumerary nuclei and sometimes axonal sprouts can be seen extending along the axon through myelin-free regions (Fig. 2C).

Muscle whole mount preparations were used to compare the morphological features of axons and Schwann cells at the NMJ of 5-month old periaxin null and control mice using neurofilament immunostaining together with fluorescent conjugates of α–BTX. In WT muscles, motor axons approach the muscle fibre and branch extensively close to the neuromuscular junction; in this region, they form terminal specializations that lie in register with AchR (Fig. 3A). In contrast, NMJs of periaxin prx−/− mice display extensive pre-terminal branching of motor axons with branch points often located at considerable distances from the endplate (Fig. 3B and C and see below). Most of these supernumerary branches converged on the same NMJ as their parent motor axon. Other abnormalities were also regularly detected in pre-terminal axons of periaxin null mice, including thinning of axon branches and focal swellings (Fig. 3C).

The increased pre-terminal branching and extended branch point distance from the terminal of prx−/− compared with WT motor axons were quantified by measuring the distance from the end-plate to nearest branch point, including only branches extending to the same NMJ, and by counting the number of branches approaching the neuromuscular junction (n=3 for 5-month old WT and prx−/− mice, 50 NMJs analysed per group). Prx−/− motor axons displayed on average 3.1±0.2 branches approaching the endplate compared with 1.2±0.1 branches in WT (mean ± SEM, Fig. 3D), a threefold difference (t-test, $p<0.001$). The distance of the most proximal branch point in prx−/− motor axons was even more marked: 34.3±2.8 μm compared with 4.7±1.8 μm in WT axons, about a sevenfold difference (t-test, $p<0.001$; Fig. 3E). Despite the increase in preterminal axonal branching, the size of

endplates in periaxin prx−/− was not significantly different from those in the WT mice (data not shown).

To discriminate if the abnormal pattern of innervation observed in periaxin null NMJs arise during neuromuscular development or at later stages, we used the same methods to examine 3-week old WT and prx−/− neuromuscular junctions. In these preparations, the morphology and pattern of innervation of WT and prx−/− motor axons were indistinguishable (Fig. 4A) and this was corroborated by the same kind of quantitative analysis described above (Fig. 4B and C).

Since neither motor nerve terminals nor perisynaptic (terminal) Schwann cells normally express periaxin (Fig. 1A), the morphological changes in prx−/− motor axons must have been an indirect consequence of the loss of periaxin from myelin forming Schwann cells in axon branches located proximal to the endplate.

Axonal abnormalities associate with pre-terminal demyelination events

The abnormal pattern of innervation in periaxin prx−/− motoraxons arises after normal formation of the neuromuscular junction and is probably related to pre-terminal demyelination. To test this possibility, 5-month old WT and prx−/− muscles were immunostained with antibodies against the myelin protein P0 and neurofilament together with AchR staining. In WT neuromuscular junctions, the last myelinated region of the nerve fibre is located before the terminal branch (Fig. 5A). In prx−/− nerve fibres, abnormal pre-terminal branches located far from the terminal were always associated with demyelinated regions (Fig. 5B) that evidently arose during the progression of the periaxin null mice condition (Fig. 4). In addition, axonal swellings immunopositive for neurofilaments, the other hallmark of periaxin null pre-terminal axons, associates with residually-myelinated regions of the nerve fibre (Fig. 5C and D).

During reinnervation and muscle paralysis, terminal Schwann cells (tSC) become “activated” and extend processes that stimulate and guide axonal sprouting (Mehta et al., 1993; Son and Thompson, 1995). To investigate if tSC reaction may underlie the pre-terminal generation of axonal sprouts that finally innervate the NMJ, terminal Schwann cells from WT and prx−/− end-plates were visualized by immunostaining with an antibody against the cytoplasmic protein S100. In WT muscles, terminal Schwann cells cap presynaptic terminals and lie in strict register with postsynaptic Ach receptors (Figure 6A). In all periaxin null NMJs examined (n=50), tSCs lay in register with the postsynaptic specialization and no sprouting was detected beyond this area, as in NMJ of WT mice (Figure 6A and B). In addition, tSC in periaxin null neuromuscular junctions did not express nestin, a marker protein of the “activated” state of terminal Schwann cells ((Hayworth et al., 2006); Figure 6C-E).

Electrophysiological consequences of peripheral demyelination revealed by high frequency stimulation

To investigate if the morphological abnormalities in periaxin null neuromuscular junctions described above result in physiological changes of neuromuscular transmission, vital

staining with FM1-43 and intracellular recording from muscle fibres were performed in acutely dissected TS and flexor digitorum brevis (FDB) muscles.

Active regions of the nerve terminal were identified by vital staining using FM1-43, which incorporates in recycling synaptic vesicles (Betz et al., 1992; Ribchester et al., 1994) and can be detected by fluorescence microscopy. TS muscles from 5-month old WT and prx−/− mice were dissected in physiological solution and active terminals were loaded with FM1-43 and stained with α-BTX. In WT neuromuscular junctions, active regions of the nerve terminal, revealed by FM1-43 staining, cover the complete area of AchR staining (Fig. 7A). In prx−/− muscles vital staining revealed no activity-related abnormalities of nerve terminals located above the AchR region (Fig. 7A). Thus, synaptic vesicle recycling was dot discernibly impaired in these mice.

Intracellular end-plate potential (EPP) recordings were made from FDB muscles. EPPs obtained after low frequency stimulation (1 Hz) were recorded from 2, 4, and 8-month old WT and prx−/− muscles (n=3 for each group) and analysed. Most mutant junctions showed normal synaptic responses, with similar amplitude, time course and quantal content compared to WT at all ages examined (Fig. 7B and data not shown). However, the EPP latency, measured from the stimulus artifact to the start of the rising EPP phase, was increased significantly in prx−/− compared with WT end-plates (Fig. 7C). By 8 months, it was 6.31 ± 0.21 milliseconds (ms) in prx−/− muscles (mean ± S.E.M) compared with 2.56 ± 0.06 ms in WT, a twofold difference ($P<0.0001$, t-test). The amplitude and frequency of spontaneous miniature end-plate potentials (MEPPs) were also similar comparing 8-month old WT and prx−/− neuromuscular synapses (Fig. 7D), suggesting normal ACh receptor distribution and function and unimpaired presynaptic regulation of spontaneous synaptic vesicle exocytosis in prx−/− mice.

Branch points are known to exhibit a low safety factor for the conduction of the action potential in myelinated and unmyelinated axons, especially when subjected to high frequency stimulation (Grossman et al., 1979a, b; Zhou and Chiu, 2001). We therefore stimulated FDB muscles via their nerve supply at a frequency of 30 Hz for 1 second; that is, well below the physiological range of *in vivo* motor axon firing frequencies (Grimby and Hannerz, 1977). At this frequency, end-plates from 8-month old WT mice respond to every incoming action potential. In contrast, 40% of prx−/− end-plates responded intermittently when stimulated at the same frequency (Fig. 8), indicating a frequency dependent block of action potential transmission. These failures cannot be explained by a reduced quantal content, since the coefficient of variation in the amplitude of EPP's that were evoked by stimulation was not significantly different from normal. Interestingly, synaptic transmission at 20 Hz was evidently sufficient to enable labelling of terminals with FM1-43 (see above)

Thus, at low stimulation frequencies neuromuscular transmission in prx−/− muscles is not compromised by the morphological abnormalities present in pre-terminal axons, including the extensive branching and swelling of the preterminal axons. However, these junctions are significantly compromised in their ability to transmit neuromuscular activity at frequencies at or above 30Hz.

Europe PMC Funders Author Manuscripts

Europe PMC Funders Author Manuscripts

Discussion

In this study we have shown that in a mouse model of CMT disease, late onset demyelination of intramuscular nerve fibres leads to a dramatic increase in nerve branches approaching individual neuromuscular junctions, in addition to axonal defects such as neurofilament-positive pre-terminal swellings and axonal thinning. To our knowledge this is the first report showing important changes at the NMJ due to demyelination and not associated with developmental abnormalities in myelin formation, such as those associated with the overexpression of the myelin protein P0 (Yin et al., 2004). The axonal abnormalities we have reported here in prx−/− axons add to the increasing evidence that myelin, in addition to its role in conduction of the action potential, is required for the integrity of the axon in the nerve fibre and neuromuscular junction. In addition, the results reported here suggest that NMJ defects may underlie clinical disabilities associated with demyelinating conditions, and should be considered in the study and treatment of demyelinating conditions.

The electrophysiological data obtained from prx−/− neuromuscular junctions revealed intermittent failure of action potential propagation only at high stimulation frequencies. At low stimulation frequency, the transmission of the action potential in periaxin null neuromuscular junctions is similar to WT in terms of end-plate potential amplitude and time course. Only a decrease in conduction velocity is detected in prx−/− neuromuscular preparations probably reflecting the extent of demyelination in the nerve fibre. In WT nerves, internodal lengths decreases in myelinated nerve fibres approaching the terminal arborisation (Quick et al., 1979), and probably reflects a physiological adaptation that increases the safety factor for action potential propagation across branch points. Interestingly, internodal length is also reduced in the myelinated regions of prx−/− nerves, which also leads to reduced nerve conduction velocity (Court et al., 2004). The intermittent failure of synaptic transmission at higher stimulation frequencies is consistent with intermittent nerve conduction block. Block of action potential conduction could occur in demyelinated segments of periaxin null nerve fibres or in preterminal regions of the axon, which show abnormal swellings and branching in the prx−/− mice. We favour the hypothesis of branch-point failure in these abnormal regions, as axonal branch points represent regions with a relatively low safety factor for conduction of the action potential, known to lead to propagation failures at high frequency stimulation (Grossman et al., 1979a, b; Zhou and Chiu, 2001).

Demyelination in periaxin null mice is a late onset event, a condition that permits study of the consequences of demyelination in NMJ structure and function without an underlying developmental defect during NMJ formation. Moreover, a possible involvement of terminal Schwann cell in abnormalities detected is ruled out due to their lack of periaxin expression in WT NMJs (Fig. 1).

Neuromuscular junctions in 3-week old periaxin prx−/− mice are innervated normally as revealed by immunofluorescence and quantification of their innervation pattern, consistent with the observation that nerves fibres from 3-week old periaxin null mice are normally myelinated and only display a reduction in Schwann cell internodal lengths (Court et al.,

2004). In addition, the normal organisation of 3-week old periaxin null neuromuscular junctions indicates that the decrease in nerve conduction velocity as a results of short internodal distances (Court et al., 2004) have no overt effects on the structure and function of the peripheral synapse.

In older prx−/− mice, demyelination takes place in nerves fibre segments proximal to the neuromuscular junction and axonal sprouts originating from these demyelinated regions leads to an increase in branches invading the endplate. Axonal processes associated with demyelinated segments are also detected in some nerve fibres located in the nerve (Fig. 2C) but not as extensive as near neuromuscular junctions.

Our observation of motor axon branching from demyelinated regions supports the long held notion that the sprouting capacity of axons is inhibited by differentiated Schwann cells. It has been shown that this repression is abolished when Schwann cells dedifferentiate (Alvarez et al., 1995; Moreno et al., 1996), are removed (Court and Alvarez, 2000) or following down-regulation of myelin proteins (Gupta et al., 2006). One candidate for this inhibitory effect on axonal sprouting is the myelin associated glycoprotein (MAG), which has been shown to inhibit both axonal regeneration and sprouting in the PNS and CNS (McKerracher et al., 1994; Li et al., 1996; Shen et al., 1998; Wong et al., 2003). It will be interesting to evaluate whether the absence of MAG in null mice leads to supernumerary branches near NMJs as described here.

The fact that supernumerary branches in periaxin-null mice innervate the same NMJ as their parent axon, but do not sprout to adjacent muscle fibres (i.e. there is no polyneuronal innervation) suggest that branches originating in demyelinated pre-terminal axonal regions are somehow constrained in their growing pathway along their parent axonal axis. In other conditions such as partial denervation or muscle inactivity, “activated” terminal Schwann cells (tSC) extend processes that guide axonal processes to adjacent denervated or paralysed motor endplates (Mehta et al., 1993; Son and Thompson, 1995). In periaxin prx−/− mice, NMJs exhibiting extensive pre-terminal branches showed terminal Schwann cells that were still restricted to the end-plate region and that did not extend processes or express nestin, a protein upregulated in activated tSC (Hayworth et al., 2006). This suggests that the phenomenon of self-reinnervation described here is independent of tSC activation.

Another interesting issue is the accommodation in the endplate of terminal specializations produced by extra branches. This process takes place in the adult prx−/− mice during nerve fibre demyelination after normal neuromuscular development. Since the area of motor endplates was normal, we may conclude that the convergence of additional branches from the same axon led to competition between branches originating from the same motor axon, with elimination of extant terminal synaptic boutons. Synaptic competition at the NMJ is regulated by activity-dependent and activity-independent processes (Costanzo et al., 2000; Buffelli et al., 2004). The endogenous activity of the convergent branches in prx−/− mouse NMJ is likely to be wholly synchronous at low frequencies of endogenous activation but to break down and become asynchronous or absent at some junctions with high frequency activation (Fig 7). It would therefore be interesting to determine to what extent

desynchronisation of activity patterns in the convergent inputs determines whether the convergent inputs are sustained or withdrawn.

Other abnormalities detected in preterminal axons of periaxin null mice are neurofilament-rich axonal swellings. These structures were associated with segments of the axon still myelinated. Axonal swellings have been described in multiple sclerosis lesions (Trapp et al., 1998), a chronic inflammatory demyelinating disease of the CNS, and in axons of mice lacking the protolipid protein (PLP) a component of the myelin formed by oligodendrocytes in the CNS (Griffiths et al., 1998). In addition, the presence of axonal swelling has been reported in motor axons of intramuscular nerves from biopsies of patient with diverse peripheral neurophaties, these axonal enlargements were not associated with signs of axonal degeneration (Alderson, 1992). In PLP null mice, axonal swellings are characterised by the accumulation of dense bodies, organelles and membranous vesicles, suggesting that defects in axonal transport may underlie the formation of swellings (Griffiths et al., 1998). In periaxin null mice, abnormal axonal transport in the interface between myelinated and demyelinated regions might be responsible for the accumulation of neurofilaments and other transported cargoes. In addition, it is well known that myelin regulates axonal caliber by inducing neurofilament phosphorylation (de Waegh et al., 1992). Therefore, swellings in prx −/− axons might represent an abnormal regulation of neurofilament phosphorylation in residually–myelinated regions. The study of preterminal axon ultrastructure and analysis of neurofilament phosphorylation state will be necessary to resolve the contribution of axonal transport defects and neurofilament phosphorylation in the formation of axonal swelling in their preterminal regions.

Materials and Methods

Mice

Generation of peraxin null mice has been previously reported (Gillespie et al., 2000). All procedures performed in animals were carried out following UK Government Home Office regulations.

Teased nerve fibres immunohistochemistry

Quadriceps and sciatic nerves were dissected and immersion fixed in 4% paraformaldehyde in 0.1M phosphate buffer saline (PBS, pH 7.4) for 45 minutes. After washing in PBS, the perineurium was dissected and nerve fibre bundles were separated using a pair of acupunture needles on a PBS drop in 3-aminopropyltriethoxysilane (Sigma) coated slides. After teasing, the slide was dried at room temperature and stored at −80 celsius degrees (°C) until use. Slides stored at −80 °C were immersed into pre-chilled (−20 °C) acetone for 20 minutes. The acetone was air dried and teased fibres were blocked/permeabilised with 0.1% Triton, 5% fish skin gelatine (Sigma) in PBS for 1 hour at room temperature. First antibodies were applied in the same blocking/permeabilising solution overnight at room temperature in a humid chamber. Subsequently, fibres were washed in PBS, 0.1% Triton X-100. Secondary antibodies were applied in blocking/permeabilizing solution for 1.5 hours at room temperature. After washing in PBS, teased fibres were mounted in Vectashield (Vector Labs, Burlingame, California).

Muscle tissue immunohistochemistry

For whole muscle preparations, muscles were dissected in 0.1 M phosphate buffer solution (PBS, pH 7.4) and fixed in 4% paraformaldehyde for 20 minutes, following by incubation in 5 μg/ml of TRITC or AlexaFluor-647 alpha-bungarotoxin (Molecular Probes) for 30 minutes. After washing in PBS and blocked/permeabilised for one hour in 1% BSA, 0.4% lysine, 0.5% Triton X-100 in PBS, primary antibodies were applied overnight at 4 °C. Muscles were washed and secondary antibodies were incubated for 3.5 hours at room temperature following by extensive washes for 1 hour and mounted in Vectashield.

Image acquisition

Immunofluorescence stainings of teased fibres and whole mount muscles were imaged using a BioRad Radiance 2000 (Nikon Eclipse E600-FN microscope) confocal system. Quantifications were performed using Image J Software (downloadable from http://rsb.info.nih.gov/ij/)

Intracellular recording from muscle fibres

Periaxin null and C57Bl/6 mice aged 7 weeks to 11 months were killed by cervical dislocation and flexor digitorum brevis (FDB) muscle were dissected in mammalian physiological solution (MPS; 120 mM NaCl, 5 mM KCl, 2 mM CaCl2, 1 mM MgCl2, 23.8 mM NaHCO3, 5.6 mM D-glucose), bubbled with O2/CO2 (95%/5%). Muscle/nerve preparation was pinned in a sylgard coated recording chamber continually perfused with MBS. The nerve was placed in a suction electrode and a pulled microelectrode was used to record end-plate potentials (EPPs) after blocking muscle action potentials for 20 minutes with μ-conotoxin (2 μM).

Styryl dye staining of motor axon terminals

Recycling synaptic vesicles in TS motor nerve terminals from WT and periaxin null mice were stained using the vital aminostyryl dye FM1-43 (Molecular Probes). Nerve muscle preparations in MPS were incubated with 5 μM FM1-43 for 5 minutes. The nerve was stimulated by a suction electrode by pulses at 20Hz, 10V, 0.1ms bandwidth for 10 minutes. Following nerve stimulation, the nerve/muscle preparations were washed in MPS for 30 minutes. After washing, postsynaptic receptors were stained with 5 μg/ml of fluorescent-conjugated alpha-bungarotoxin for 10 minutes in MPS, washed for 10 minutes and observed using fluorescent microscopy.

Primary and secondary antibodies

The following antibodies, sources and dilutions were used in the present study. Mouse IgG1 anti-nestin, S. Hockfield, 1:200; mouse anti-neurofilament (165 kDa), DHSB, 1:200; mouse IgG1 anti-neurofilament (200 kDa), Sigma, 1:1000; rabbit anti-periaxin, P. J. Brophy, 1:3000; rabbit anti-S100, DAKO, 1:200; mouse anti-SV2, SAPU, 1:200; rabbit anti-P0, T. Brookes, 1:400. Goat TRITC-conjugated anti-mouse IgG, Southern Biotech, 1:200; donkey FITC-conjugated anti-rabbit IgG, Jackson, 1:200; goat AlexaFluor-647-conjugated anti-mouse IgG1, Molecular Probes, 1:100. Goat AlexaFluor-647-conjugated anti-rabbit IgG, Molecular Probes, 1:100.

Europe PMC Funders Author Manuscripts

Acknowledgements

This work was supported by grants from the MRC and the Wellcome Trust.. We are grateful to Mr Derek Thomson, Mr Adrian Thomson and Ms Linda Ferguson for expert technical assistance.

References

Alderson K. Axonal swellings in human intramuscular nerves. Muscle Nerve. 1992; 15:1284–1289. [PubMed: 1488067]

Alvarez J, Moreno RD, Inestrosa NC. Mitosis of Schwann cells and demyelination are induced by the amyloid precursor protein and other protease inhibitors in the rat sciatic nerve. Eur J Neurosci. 1995; 7:152–159. [PubMed: 7536093]

Betz WJ, Mao F, Bewick GS. Activity-dependent fluorescent staining and destaining of living vertebrate motor nerve terminals. J Neurosci. 1992; 12:363–375. [PubMed: 1371312]

Bjartmar C, Yin X, Trapp BD. Axonal pathology in myelin disorders. J Neurocytol. 1999; 28:383–395. [PubMed: 10739578]

Buffelli M, Busetto G, Bidoia C, Favero M, Cangiano A. Activity-dependent synaptic competition at mammalian neuromuscular junctions. News Physiol Sci. 2004; 19:85–91. [PubMed: 15143199]

Costanzo EM, Barry JA, Ribchester RR. Competition at silent synapses in reinnervated skeletal muscle. Nat Neurosci. 2000; 3:694–700. [PubMed: 10862702]

Court F, Alvarez J. Nerve regeneration in Wld(s) mice is normalized by actinomycin D. Brain Res. 2000; 867:1–8. [PubMed: 10837792]

Court FA, Alvarez J. Local regulation of the axonal phenotype, a case of merotrophism. Biol Res. 2005; 38:365–374. [PubMed: 16579519]

Court FA, Sherman DL, Pratt T, Garry EM, Ribchester RR, Cottrell DF, Fleetwood-Walker SM, Brophy PJ. Restricted growth of Schwann cells lacking Cajal bands slows conduction in myelinated nerves. Nature. 2004; 431:191–195. [PubMed: 15356632]

de Waegh SM, Lee VM, Brady ST. Local modulation of neurofilament phosphorylation, axonal caliber, and slow axonal transport by myelinating Schwann cells. Cell. 1992; 68:451–463. [PubMed: 1371237]

Dyck, PJ.; Thomas, PK. Peripheral neurophaty. Elsevier; New York: 2005. p. 2992

Garcia A, Combarros O, Calleja J, Berciano J. Charcot-Marie-Tooth disease type 1A with 17p duplication in infancy and early childhood: a longitudinal clinical and electrophysiologic study. Neurology. 1998; 50:1061–1067. [PubMed: 9566395]

Gillespie CS, Sherman DL, Fleetwood-Walker SM, Cottrell DF, Tait S, Garry EM, Wallace VC, Ure J, Griffiths IR, Smith A, Brophy PJ. Peripheral demyelination and neuropathic pain behavior in periaxin-deficient mice. Neuron. 2000; 26:523–531. [PubMed: 10839370]

Griffiths I, Klugmann M, Anderson T, Yool D, Thomson C, Schwab MH, Schneider A, Zimmermann F, McCulloch M, Nadon N, Nave KA. Axonal swellings and degeneration in mice lacking the major proteolipid of myelin. Science. 1998; 280:1610–1613. [PubMed: 9616125]

Grimby L, Hannerz J. Firing rate and recruitment order of toe extensor motor units in different modes of voluntary contraction. J Physiol. 1977; 264:865–879. [PubMed: 845828]

Grossman Y, Parnas I, Spira ME. Mechanisms involved in differential conduction of potentials at high frequency in a branching axon. J Physiol. 1979a; 295:307–322. [PubMed: 521940]

Grossman Y, Parnas I, Spira ME. Differential conduction block in branches of a bifurcating axon. J Physiol. 1979b; 295:283–305. [PubMed: 521937]

Guilbot A, Williams A, Ravise N, Verny C, Brice A, Sherman DL, Brophy PJ, LeGuern E, Delague V, Bareil C, Megarbane A, Claustres M. A mutation in periaxin is responsible for CMT4F, an autosomal recessive form of Charcot-Marie-Tooth disease. Hum Mol Genet. 2001; 10:415–421. [PubMed: 11157804]

Gupta R, Rummler LS, Palispis W, Truong L, Chao T, Rowshan K, Mozaffar T, Steward O. Local down-regulation of myelin-associated glycoprotein permits axonal sprouting with chronic nerve compression injury. Exp Neurol. 2006; 200:418–429. [PubMed: 16764860]

Gutmann L, Fakadej A, Riggs JE. Evolution of nerve conduction abnormalities in children with dominant hypertrophic neuropathy of the Charcot-Marie-Tooth type. Muscle Nerve. 1983; 6:515–519. [PubMed: 6314135]

Hayworth CR, Moody SE, Chodosh LA, Krieg P, Rimer M, Thompson WJ. Induction of neuregulin signaling in mouse schwann cells in vivo mimics responses to denervation. J Neurosci. 2006; 26:6873–6884. [PubMed: 16793894]

Kabzinska D, Drac H, Sherman DL, Kostera-Pruszczyk A, Brophy PJ, Kochanski A, Hausmanowa-Petrusewicz I. Charcot-Marie-Tooth type 4F disease caused by S399fsx410 mutation in the PRX gene. Neurology. 2006; 66:745–747. [PubMed: 16534116]

Krajewski KM, Lewis RA, Fuerst DR, Turansky C, Hinderer SR, Garbern J, Kamholz J, Shy ME. Neurological dysfunction and axonal degeneration in Charcot-Marie-Tooth disease type 1A. Brain. 2000; 123(Pt 7):1516–1527. [PubMed: 10869062]

Li M, Shibata A, Li C, Braun PE, McKerracher L, Roder J, Kater SB, David S. Myelin-associated glycoprotein inhibits neurite/axon growth and causes growth cone collapse. J Neurosci Res. 1996; 46:404–414. [PubMed: 8950700]

Martini R. Animal models for inherited peripheral neuropathies. J Anat. 1997; 191(Pt 3):321–336. [PubMed: 9418989]

Martini R. The effect of myelinating Schwann cells on axons. Muscle Nerve. 2001; 24:456–466. [PubMed: 11268016]

McKerracher L, David S, Jackson DL, Kottis V, Dunn RJ, Braun PE. Identification of myelin-associated glycoprotein as a major myelin-derived inhibitor of neurite growth. Neuron. 1994; 13:805–811. [PubMed: 7524558]

Mehta A, Reynolds ML, Woolf CJ. Partial denervation of the medial gastrocnemius muscle results in growth-associated protein-43 immunoreactivity in sprouting axons and Schwann cells. Neuroscience. 1993; 57:433–442. [PubMed: 8115047]

Moreno RD, Inestrosa NC, Culwell AR, Alvarez J. Sprouting and abnormal contacts of nonmedullated axons, and deposition of extracellular material induced by the amyloid precursor protein (APP) and other protease inhibitors. Brain Res. 1996; 718:13–24. [PubMed: 8773762]

Quick DC, Kennedy WR, Donaldson L. Dimensions of myelinated nerve fibers near the motor and sensory terminals in cat tenuissimus muscles. Neuroscience. 1979; 4:1089–1096. [PubMed: 492526]

Ribchester RR, Mao F, Betz WJ. Optical measurements of activity-dependent membrane recycling in motor nerve terminals of mammalian skeletal muscle. Proc Biol Sci. 1994; 255:61–66. [PubMed: 8153137]

Salzer JL. Polarized domains of myelinated axons. Neuron. 2003; 40:297–318. [PubMed: 14556710]

Sancho S, Magyar JP, Aguzzi A, Suter U. Distal axonopathy in peripheral nerves of PMP22-mutant mice. Brain. 1999; 122(Pt 8):1563–1577. [PubMed: 10430839]

Shen YJ, DeBellard ME, Salzer JL, Roder J, Filbin MT. Myelin-associated glycoprotein in myelin and expressed by Schwann cells inhibits axonal regeneration and branching. Mol Cell Neurosci. 1998; 12:79–91. [PubMed: 9770342]

Sherman DL, Fabrizi C, Gillespie CS, Brophy PJ. Specific disruption of a schwann cell dystrophin-related protein complex in a demyelinating neuropathy. Neuron. 2001; 30:677–687. [PubMed: 11430802]

Son YJ, Thompson WJ. Nerve sprouting in muscle is induced and guided by processes extended by Schwann cells. Neuron. 1995; 14:133–141. [PubMed: 7826631]

Takashima H, Boerkoel CF, De Jonghe P, Ceuterick C, Martin JJ, Voit T, Schroder JM, Williams A, Brophy PJ, Timmerman V, Lupski JR. Periaxin mutations cause a broad spectrum of demyelinating neuropathies. Ann Neurol. 2002; 51:709–715. [PubMed: 12112076]

Trapp BD, Peterson J, Ransohoff RM, Rudick R, Mork S, Bo L. Axonal transection in the lesions of multiple sclerosis. N Engl J Med. 1998; 338:278–285. [PubMed: 9445407]

Wong EV, David S, Jacob MH, Jay DG. Inactivation of myelin-associated glycoprotein enhances optic nerve regeneration. J Neurosci. 2003; 23:3112–3117. [PubMed: 12716917]

Wrabetz L, Feltri ML, Quattrini A, Imperiale D, Previtali S, D'Antonio M, Martini R, Yin X, Trapp BD, Zhou L, Chiu SY, Messing A. P(0) glycoprotein overexpression causes congenital hypomyelination of peripheral nerves. J Cell Biol. 2000; 148:1021–1034. [PubMed: 10704451]

Yin X, Kidd GJ, Pioro EP, McDonough J, Dutta R, Feltri ML, Wrabetz L, Messing A, Wyatt RM, Balice-Gordon RJ, Trapp BD. Dysmyelinated lower motor neurons retract and regenerate dysfunctional synaptic terminals. J Neurosci. 2004; 24:3890–3898. [PubMed: 15084670]

Zhou L, Chiu SY. Computer model for action potential propagation through branch point in myelinated nerves. J Neurophysiol. 2001; 85:197–210. [PubMed: 11152720]

Zu Horste GM, Nave KA. Animal models of inherited neuropathies. Curr Opin Neurol. 2006; 19:464–473. [PubMed: 16969156]

Europe PMC Funders Author Manuscripts

Europe PMC Funders Author Manuscripts

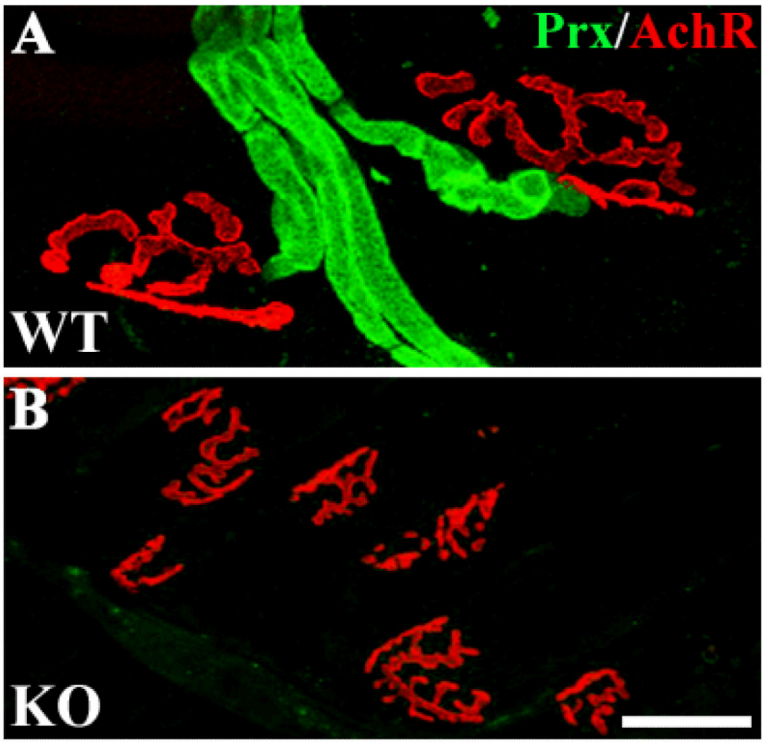

Figure 1. Periaxin expression in pre-terminal myelinated Schwann cells of intramuscular nerves

Immunostaining for periaxin protein (green) together with AChR staining (red) in wild-type **(A)** and periaxin null **(B)** TS muscle. In WT muscles, periaxin is present in myelinating Schwann cells but not in perisynaptic ones, which lies in register with the AChR. Periaxin immunoreactivity is completely absent in null TS muscle. Scale bar, 25μm and 50 μm for A and B, respectively.

Europe PMC Funders Author Manuscripts

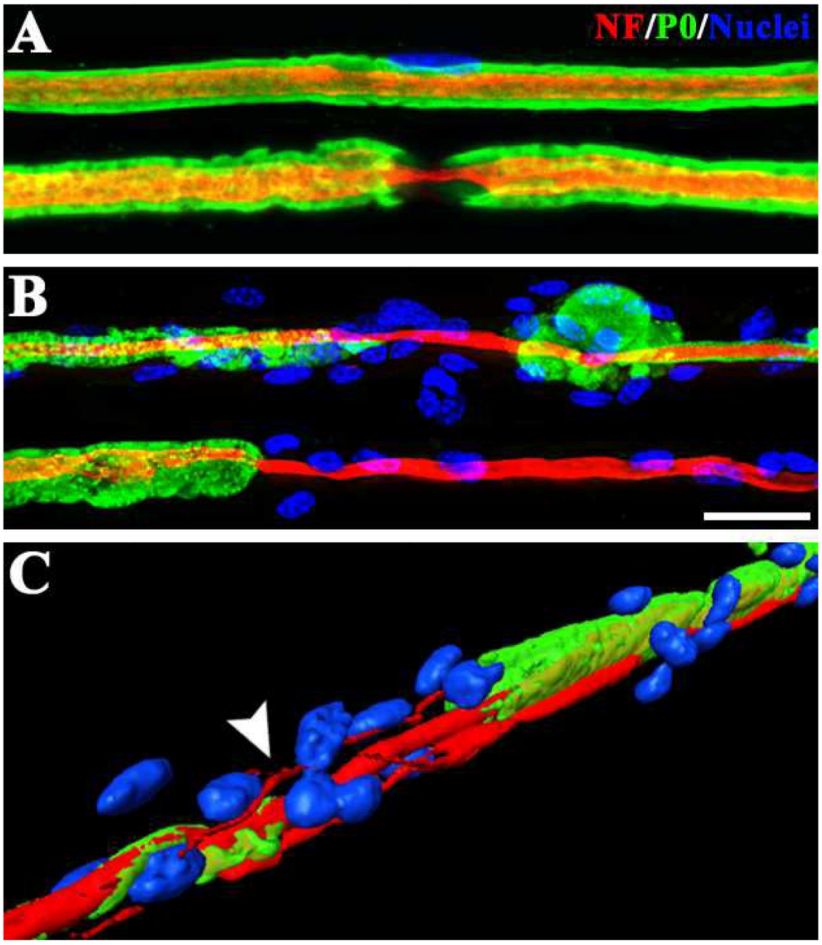

Figure 2. Peripheral demyelination in periaxin null mice

Teased sciatic nerve fibres from 8-month old wild-type **(A)** and periaxin null mice **(B)** were immunostained for the myelin protein P0 (green), neurofilaments (red) and counterstained with DAPI (blue). Periaxin null nerve fibres shown focal thickenings of the myelin sheath flanking demyelinated segments and increase in the nuclei number, corresponding to Schwann cells attempting to remyelinate demyelinated fibres. In **(C)**, a three-dimensional rendering was performed in a periaxin null teased fibre illustrating the presence of sprouts in the demyelinated segment (arrowhead). Scale bar, 20 μm.

Europe PMC Funders Author Manuscripts

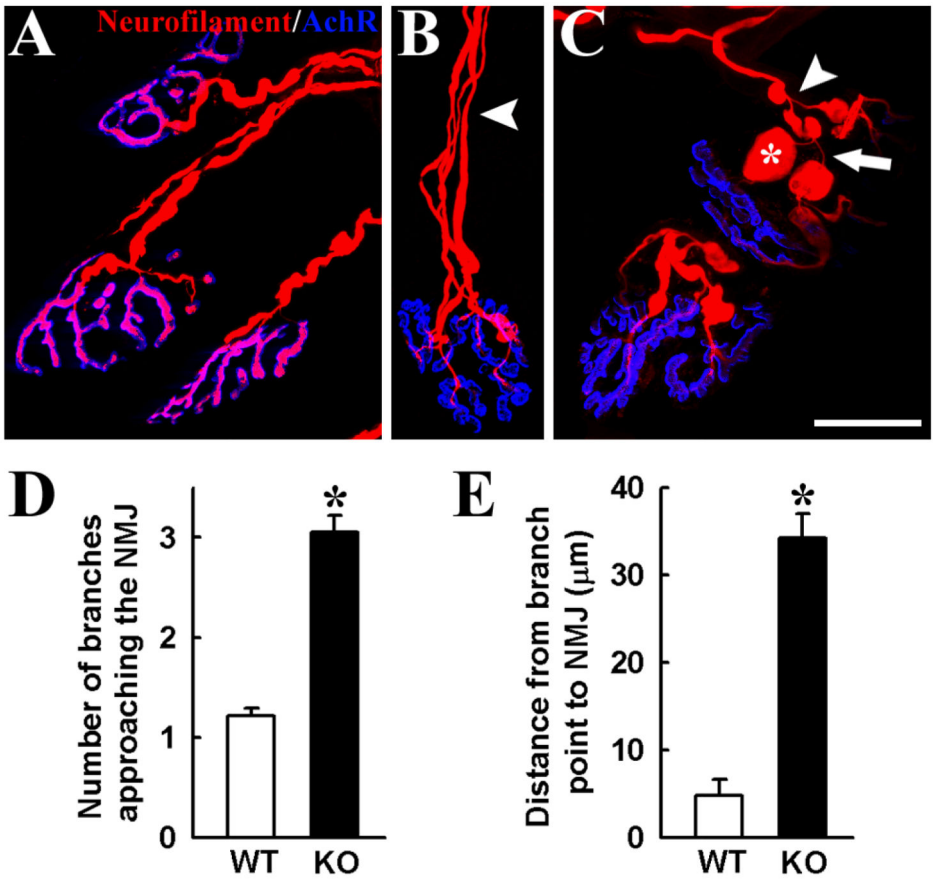

Figure 3. Motor axon abnormalities in the periaxin null mice

Immunostaining for neurofilament (red) together with AChR staining (blue) shown that in WT neuromuscular junctions motor axons branch extensively when they contact the end-plate region **(A)**. In contrast, preterminal axons of periaxin null mice exhibit several abnormalities **(B)** and **(C)**, including increased number of preterminal axon branches (arrowhead), thinning of axon branches (arrow) and focal swellings (asterisk). More than 80% of periaxin null neuromuscular junctions present these abnormalities but none of these features are found in wild-type animals. Scale bar, 30 μm. Quantification of the innervation pattern of WT and prx−/− neuromuscular junctions shown an increase in prx−/− pre-terminal branches contacting the neuromuscular junction compared with the WT values **(D)**. In addition, the distance from the proximal branch point to the neuromuscular junction is increased in prx−/− neuromuscular junctions compared with WT ones **(E)** (asterisk, t-test $p<0.001$).

Europe PMC Funders Author Manuscripts

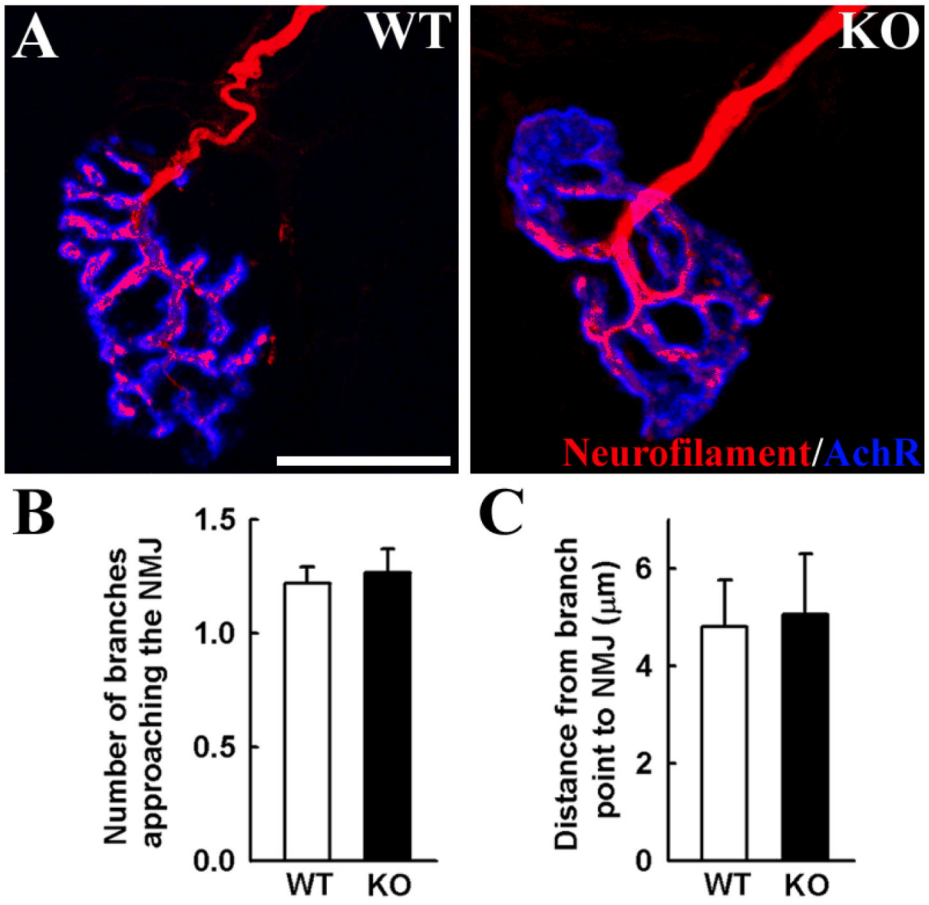

Figure 4. Periaxin null mice develop a morphologically normal neuromuscular junction

(A) In 3-week old mice, prx−/− neuromuscular junctions appear normal as revealed by immunostaining for neurofilaments (red) and AchR staining (blue). In addition, the number of branches per NMJ **(B)** and the distance from the last branch point to the end-plate **(C)** are not statistically different from WT values. Scale bar, 20 μm.

Europe PMC Funders Author Manuscripts

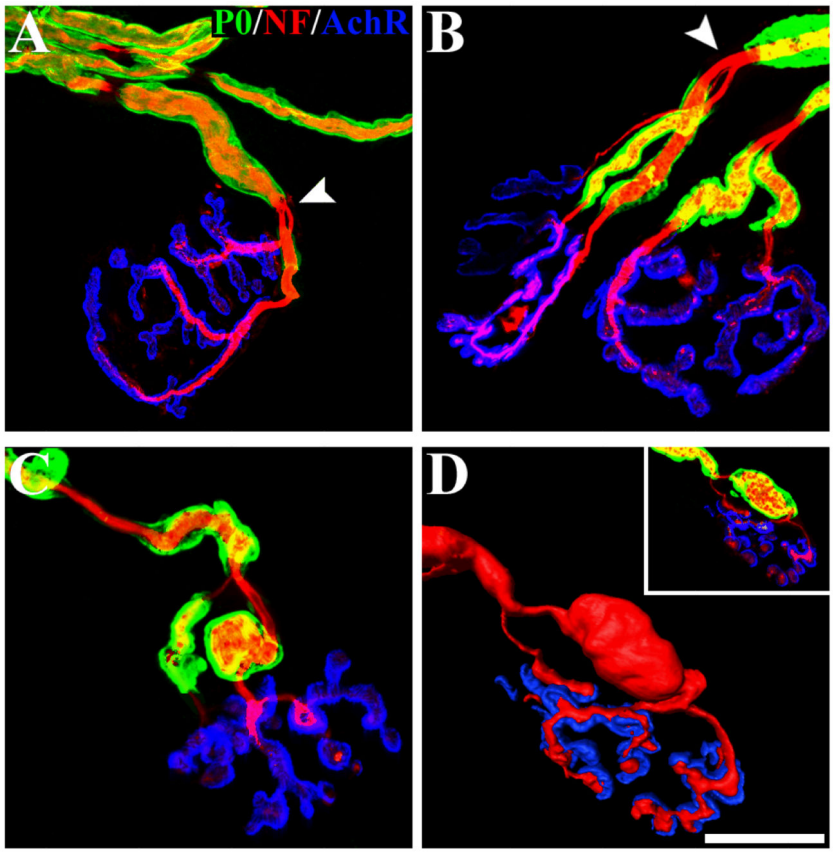

Figure 5. Axon abnormalities are related to preterminal demyelination

TS muscles from 5-month old WT and prx−/− mice immunostained for neurofilament and synaptic vesicle protein (red), myelin protein zero (P0, green) together with AChR staining (blue). In WT neuromuscular junctions, the last myelinated region occurs before the terminal branch **(A)**. In prx−/− mice, preterminal branch-points (arrowhead) are always associated with regions devoid of myelin **(B)**. In addition, neurofilament-rich swellings **(C)** are associated with residually–myelinated regions (P0-positive staining). In **(D)** a 3D rendering was performed showing that the neurofilament-positive swelling is associated with a P0 rich region (inset). Scale bar, 20 μm.

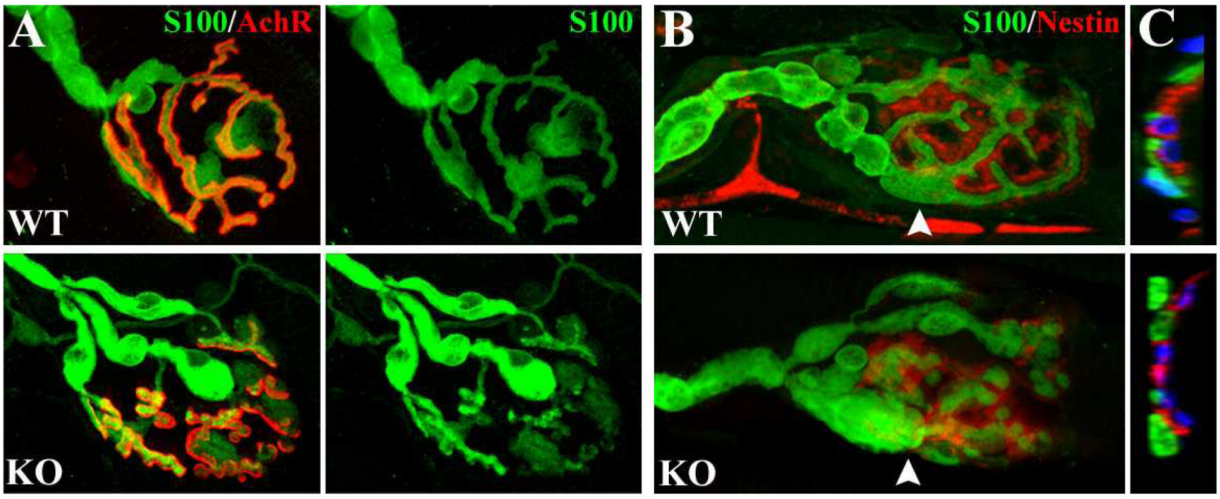

Figure 6. Perisynaptic (terminal) Schwann cells are not activated in periaxin null NMJs

TS muscles from WT (upper panels) and prx −/− (lower panels) mice immunostained for the Schwann cell protein S100 together with AchR staining **(A)** or nestin **(B)**. In both WT and Prx −/− NMJs S100 positive terminal Schwann cells lies in register with AchR staining **(A)**. Nestin, a protein expressed in activated terminal Schwann cells, is restricted to the postsynaptic region in both WT and prx −/− NMJs **(B)**. The exclusive postsynaptic localization of nestin can be better observed in Z projections **(C)** performed at the arrowhead levels indicated in **(B)**. In **(C)**, the blue signal correspond to nuclei staining. Scale bar, 20 μm.

Europe PMC Funders Author Manuscripts

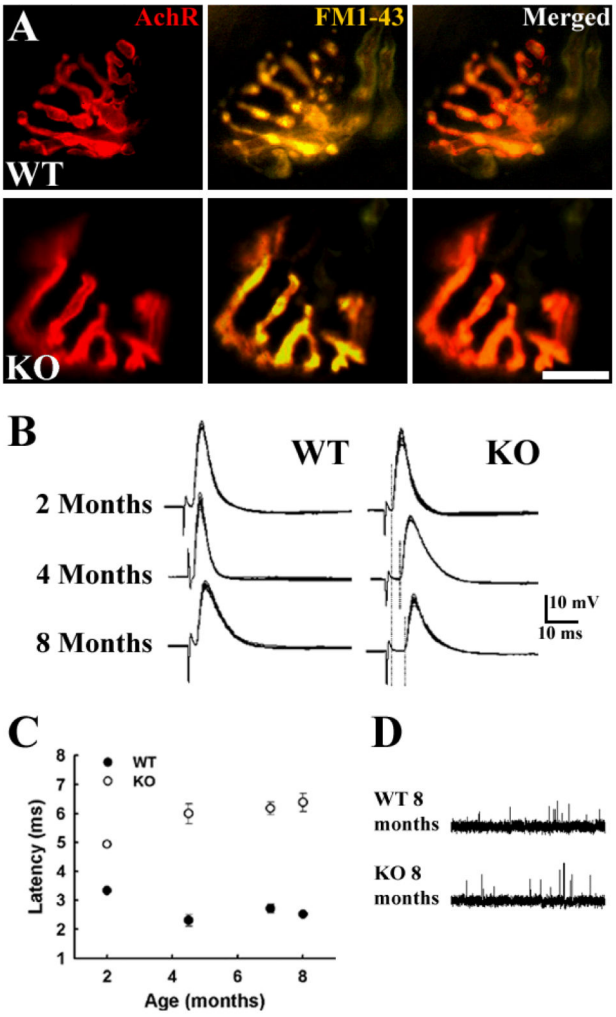

Figure 7. Periaxin null mice have normal end-plate potentials (EPPs) and miniature end-plate potentials (MEPPs) but an increase in latency

WT and prx−/− motor end plates were identified using the activity-dependent staining properties of FM1-43 and Rhodamine-α-bungarotoxin to visualise AChR in fresh preparations. This vital FM1-43 staining reveals a normal neuromuscular innervation in periaxin null neuromuscular junctions (**A**; upper panel, WT; lower panel, prx−/−). Scale bar, 20 μm. **(B)** The mean EPP peak amplitude recorded from prx−/− mice at different ages was not significantly different from the mean EPP peak amplitude recorded from the normal strain. The rise time and half decay time of synaptic potentials were also no different between mutant and control strains. **(C)** The latency of EPPs incresases with age in prx−/− muscles, probably reflecting the advancement of the demyelinating phenotype. The amplitude and frequency of spontaneous MEPPs were also equal between WT and prx−/− neuromuscular synapses **(D)**; since the quantal size reflects the post-synaptic sensitivity to acetylcholine, these data suggest that ACh receptor distribution and function are also normal.

Europe PMC Funders Author Manuscripts

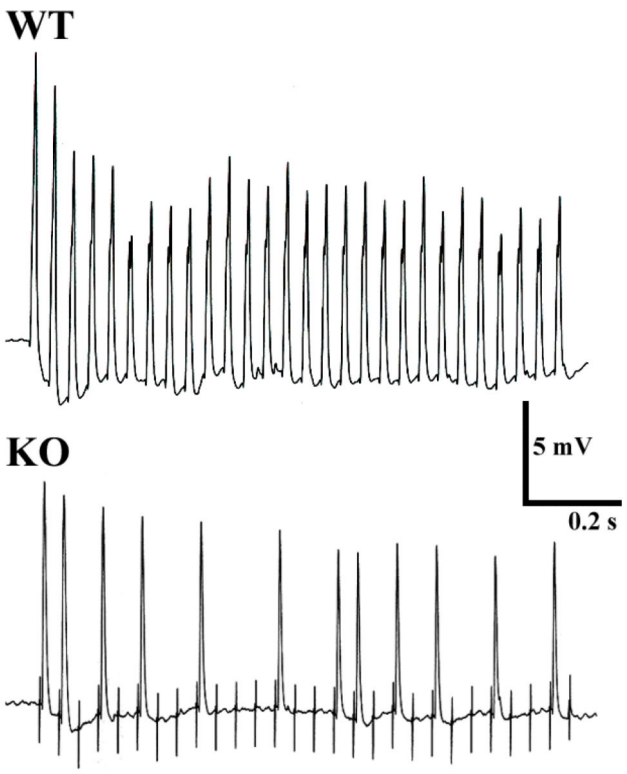

Figure 8. Periaxin null neuromuscular junctions respond intermittently to repetitive stimulation

Following stimulation at 30 Hz for 1 second, many prx−/− end plates (KO) responded only to some stimuli compared with a 100% response in the wild-type (WT) animals. This result may be related to a decrease in the safety factor for nerve conduction, perhaps as a result of increased pre-terminal branching and terminal axon demyelination. Note that the variation of EPP amplitudes in the successful responses in the lower trace was not discernibly different from wild-type, suggesting that the EPP failures at high frequency stimulation in prx−/− preparations is unlikely to be caused by any systematic reduction in the quantal content of evoked EPPs.